J. Korean Inst. Electr. Electron. Mater. Eng.
Vol. 38, No. 2, pp. 143-152 March 2025
doi: https://doi.org/10.4313/JKEM.2025.38.2.3
ISSN 1226-7945(Print), 2288-3258(Online)

Tutorial Status Report

레이저 도플러 진동계를 이용한 압전 박막의 횡 압전 계수 측정

무하마드 시라즈, 박봉찬, 안창원

울산대학교 반도체학과 에너지 하베스트-스토리지 연구소

초록: 압전 박막은 전자기기의 소형화 및 통합 시스템화로 인해 MEMS 장치, 웨어러블 전자 장치, 랩온어칩 시스템과 같은 응용 분야에서 중요하게 활용되고 있다. 압전 박막의 경우 두께 방향으로 전기 신호를 인가하더라도 전기장 방향의 수직 방향인 면 방향으로 더 큰 변형을 얻을 수 있기 때문에 압전 박막 소자는 횡 방향 모드를 활용하여 소자를 설계하는 경우가 많다. 그러므로 압전 박막은 횡 방향 압전계수를 측정하여 평가하는 것이 중요하다. 이 튜토리얼 논문은 레이저 도플러 진동계(laser Doppler vibrometry, LDV)를 사용하여 압전 박막의 유효 횡 압전 계수($e_{31,f}$)를 평가하기 위한 방법을 소개한다. 그리고 $Bi_{1/2}Na_{1/2}TiO_3$-기반 압전 박막을 예로 들어서 $e_{31,f}$을 측정하는 방법을 순서대로 정리하였다. 그러므로 이 튜토리얼 논문은 새로운 압전 박막 재료의 개발에 있어서 횡 압전 특성을 측정하고 분석하는 현실적이고 유용한 방법을 지원할 수 있을 것이다.

키워드: 유효 횡 압전 계수, 압전체, 박막, 레이저 도플러 진동계

Measurement of Transverse Piezoelectric Coefficient of Piezoelectric Thin Films Using Laser Doppler Vibrometer

Muhammad Sheeraz, Bong Chan Park, and Chang Won Ahn

Department of Semiconductor Physics and Energy Harvest-Storage Research Center (EHSRC), University of Ulsan, Ulsan 44610, Korea

(Received January 7, 2025; Revised January 16, 2025; Accepted January 17, 2025)

Abstract: Piezoelectric thin films have become increasingly significant in applications such as MEMS devices, wearable electronics, and lab-on-a-chip systems due to the miniaturization and integration of electronic devices. For piezoelectric thin films, even when an electric signal is applied in the thickness direction, greater deformation can often be observed in the in-plane direction, which is perpendicular to the electric field. Therefore, piezoelectric thin film devices are frequently designed using the transverse mode. As a result, it is crucial to evaluate piezoelectric thin films by measuring their transverse piezoelectric coefficient. This tutorial paper introduces a method for evaluating the effective transverse piezoelectric coefficient ($e_{31,f}$) of piezoelectric thin films using laser Doppler vibrometry (LDV). Additionally, the paper outlines a step-by-step procedure for measuring $e_{31,f}$ while using $Bi_{1/2}Na_{1/2}TiO_3$-based piezoelectric thin films as an example. This tutorial is expected to provide a practical and valuable method for measuring and analyzing the transverse piezoelectric properties, thereby supporting the development of new piezoelectric thin film materials.

Keywords: Effective transverse piezoelectric coefficient, Piezoelectrics, Thin film, Laser Doppler vibrometer

✉ **Chang Won Ahn; cwahn@ulsan.ac.kr**

Copyright ©2025 KIEEME. All rights reserved.
This is an Open-Access article distributed under the terms of the Creative Commons Attribution Non-Commercial License (http://creativecommons.org/licenses/by-nc/3.0) which permits unrestricted non-commercial use, distribution, and reproduction in any medium, provided the original work is properly cited.

1. INTRODUCTION

- Piezoelectrics are materials that generate electrical signals when subjected to external mechanical stress. Conversely, when an electric signal is applied to these materials, these materials undergo mechanical strain. The former phenomenon is known as the piezoelectric effect (or direct piezoelectric effect), while the latter is referred to as the converse piezoelectric effect [1].
- Piezoelectric thin films play an important role in applications demanding precise and miniaturized sensors and actuators. Compact size and compatibility with diverse substrates, the piezoelectric films enable the efficient conversion of mechanical energy into electrical signals, and vice versa, realizing them for advanced technologies such as micro-electro-mechanical systems (MEMS), wearable devices, flexible electronics, and lab-on-a-chip platforms. These films further facilitate a broad range of functionalities, including vibration sensing, energy harvesting, acoustic wave detection, and the precise manipulation of fluids in confined environments [2-4].
- Piezoelectric thin-film devices are emerging as essential components in modern electronic systems, driven by the growing need for miniaturization and multifunctionality. The versatility of these devices is well reflected in their wide-range applications, including accelerometers, RF filters, autofocus systems, pressure sensors, and gyroscopes.
- The market for MEMS devices utilizing piezoelectric thin films is expected to expand continuously, driven by the growth of smartphones, IoT, and wearable devices. Moreover, advanced devices based on piezoelectric thin films are anticipated to have a significant impact across various fields, including the rise of smart devices, the advancement of autonomous vehicles, and developments in the medical sector.
- Piezoelectric thin-film devices are employed as application components across various fields and are integrated into numerous technologies and products. Here, we summarize few examples using piezoelectric thin-film materials in application components.
  - **Piezoelectric Accelerometers** (Fig. 1): Piezoelectric accelerometers are devices that detect dynamic forces such as acceleration, vibration, and shock, converting these mechanical inputs into electrical signals. Owing to the instant sense ability of the object motion, these accelerometers are becoming essential components in various control systems, including those for automobiles, trains, ships, airplanes, factory automation, and robotics. The application fields for accelerometers are remarkably broad. Accelerometers manufactured using semiconductor technology can be classified into piezoelectric, capacitive, or piezoresistive types, depending on the transducer used to convert mechanical signals into electrical signals. While the microstructure of the transducers varies, piezoelectric accelerometers typically feature cantilever or bridge structures with a mass, as shown in Fig. 1. When an acceleration force is applied to the sensor structure, the mass displacement occurs proportionally to the magnitude of the applied acceleration. The displacement further generates an electrical signal based on the degree of movement. Compared to capacitive and piezoresistive types, piezoelectric accelerometers offer the advantage of superior sensitivity [5,6].

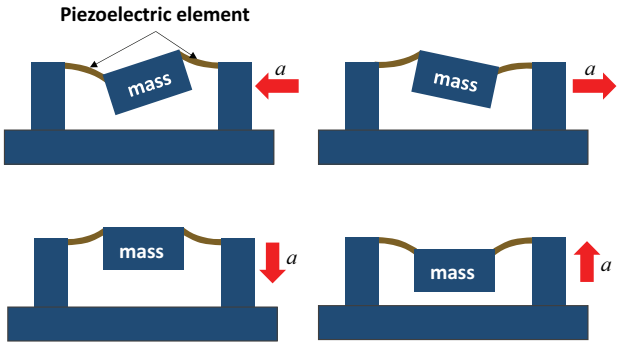

Fig. 1. (a) Working mechanism of MEMS accelerometer fabricated using a piezoelectric film.

  - **Piezoelectric Generators:** Piezoelectric materials exhibit the remarkable capability to convert external vibrations or pressure into electrical energy (Fig. 2). These characteristics preserved in piezoelectric generators play a key role in energy harvesting technologies. By producing small but crucial amounts of energy, these generators are ideal for powering devices such as military and environmental sensors, wearable health monitors, and wireless sensor networks [7,8].

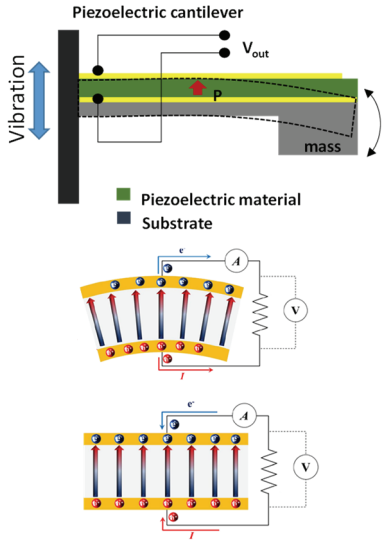

Fig. 2. Working mechanism of piezoelectric generators. Adapted with permission from [8]. Copyright 2015 AIP Publishing.

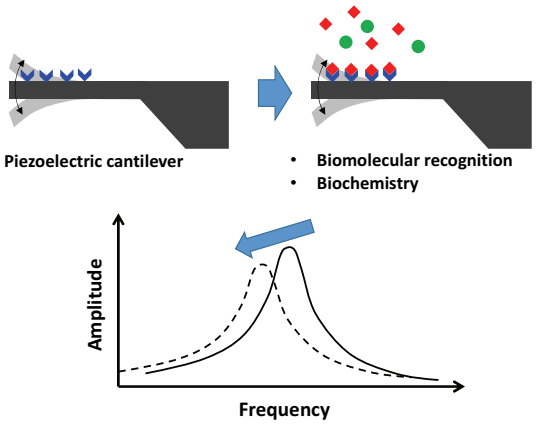

Fig. 3. Working mechanism of piezoelectric microcantilever mass sensors.

- **Piezoelectric Microcantilever Mass Sensors:** Piezoelectric microcantilever mass sensors, capable of detecting trace amounts of mass, are currently the subject of extensive research due to their potential applications in environmental monitoring, biochemical weapon detection for military and anti-terrorism purposes, and disease diagnosis. These mass sensors, based on piezoelectric materials, measure mass changes by detecting shifts in the resonance frequency. For example, a piezoelectric element produces consistent vibrations like the quartz oscillator used in electronic watches. When a substance adheres to the electrode surface of the oscillator, the increase in the mass of the substance causes a decrease in the resonance frequency. Research is actively being conducted to develop biosensors using the same principle, where substances capable of binding to specific molecules are applied to the surface of the piezoelectric material and exposed to a particular environment. The resonance frequency changes in proportion to the mass of the reacted molecules (Fig. 3). When microcantilevers are fabricated using piezoelectric thin films for mass sensing, it is possible to detect ultra-low masses in the femtogram (10^{-15} g) range. MEMS devices utilizing piezoelectric thin films are advantageous for implementing portable biosensor systems, as their small size allows for the immediate detection of biomaterials and result verification in the field, without the need for transporting samples to a laboratory. Recently, the fusion of biosensor technology and IT has been advancing in the development of real-time health and environmental monitoring technologies [9].
- **Piezoelectric MEMS Microphone** (Fig. 4)**:** A piezoelectric MEMS microphone is an acoustic sensing device that converts sound signals into electrical signals using piezoelectric materials. It offers high sensitivity, durability, and suitability for miniaturized mobile electronic devices. Unlike conventional capacitive microphones, piezoelectric MEMS microphones use piezoelectric thin films to generate electrical signals in response to mechanical vibrations caused by sound waves. Unlike traditional capacitive microphones, piezoelectric MEMS microphones perform excellently in compact designs, making them essential components in audio and sensor technological devices [10,11]. Piezoelectric MEMS microphones can generally be designed using two mechanisms: diaphragm-based or cantilever-based designs. Among these, the cantilever-based design is an ideal choice as it eliminates residual stress, which is known to significantly reduce the sensitivity of diaphragm-based microphones. Fig. 4 shows an example of a typical cantilever-based MEMS microphone design [11].

■ It is necessary to study piezoelectric thin film devices and measure and analyze the piezoelectric properties of corresponding films [12-16].

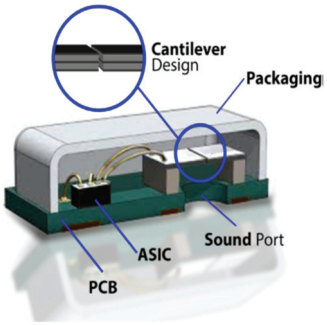

Fig. 4. Example of a typical cantilever-based MEMS microphone design. Adapted with permission from [11]. Copyright 2022 Elsevier.

- When evaluating the piezoelectric properties of the materials, the piezoelectric coefficients can be measured and assessed depending on the shape of the device and the piezoelectric mode used, such as the longitudinal mode (d_{33}), transverse mode (d_{31}), and shear mode (d_{15}).
- Generally, for bulk ceramic devices, piezoelectric properties are typically assessed by measuring the strain produced in the direction of an applied electric field after polarization alignment or by applying pressure along the polarization direction and quantifying the charge generated in the same direction to determine the longitudinal piezoelectric coefficient (d_{33}).
- In the case of piezoelectric thin films, since the length in the plane direction is much larger than the thickness of the film, even when an electric signal is applied in the thickness direction, a larger deformation occurs in the in-plane direction, which is perpendicular to the electric field direction. Therefore, piezoelectric thin film devices are often designed to utilize the transverse mode. As a result, it is important to evaluate piezoelectric thin films by measuring the transverse piezoelectric coefficient (d_{31}).
- To calculate d_{31}, the elastic coefficients, such as the Young's modulus of the piezoelectric thin film, are generally required. However, it is challenging to measure/determine the elastic coefficients of thin film materials. On the other hand, the transverse piezoelectric coefficient e_{31} is almost independent of the elastic coefficients of the piezoelectric thin film. Therefore, e_{31} is primarily measured and analyzed when evaluating the piezoelectric properties of thin films.
- The piezoelectric coefficient e is commonly referred to as the piezoelectric stress coefficient (or constant). It represents the relationship, as shown in Equation (1), between dielectric displacement D (or the amount of electric charge generated on the surface of a piezoelectric material) and the strain S in the piezoelectric material, or between mechanical stress T and an externally applied electric field E in the material. As is well known, the former describes the direct piezoelectric effect, while the latter represents the inverse piezoelectric effect [17-20].

$$e = \left(\frac{\partial D}{\partial S}\right)_E = -\left(\frac{\partial T}{\partial E}\right)_S \quad (1)$$

- The piezoelectric stress coefficient (e) is related to the piezoelectric charge coefficient (d) and the elastic compliance (s) through the relationship shown in Equation (2). Therefore, it is useful for evaluating the piezoelectric properties in devices with piezoelectric thin films, especially when it is difficult to measure the elastic modulus of the piezoelectric material [17,21].

$$e_{ij} = d_{ik}/s_{kj} \quad (2)$$

- Since piezoelectric thin films are fixed to the substrate plane, the e_{ij} coefficients of the films differ from those of conventional bulk ceramics. Therefore, the transverse piezoelectric coefficient e_{31} measured for the thin film is referred to as the " effective transverse piezoelectric coefficient" and is abbreviated as $e_{31,f}$ or $e_{31,eff}$.
- A method for measuring the transverse piezoelectric coefficient related to the direct piezoelectric effect is to induce strain in a wafer with a deposited piezoelectric film in several ways, and then calculate $e_{31,f}$ by measuring the strain and generated charge of the piezoelectric film. Methods for generating strain in a piezoelectric film sample include using an air pressure chamber, a dual-ring, or a four-point bending device [22-25].
- The method for measuring the transverse piezoelectric coefficient $e_{31,f}$ associated with the inverse piezoelectric effect involves fabricating the piezoelectric thin film deposited on a substrate and then designing it into a cantilever structure. An electric field is applied to the fabricated cantilever, and the displacement at the tip of the cantilever is measured. The transverse piezoelectric coefficient $e_{31,f}$ is then calculated using the applied voltage

and the displacement at the tip of the cantilever [21,26,27].

- This tutorial paper introduces the experimental setup for evaluating the effective transverse piezoelectric coefficient ($e_{31,f}$) of piezoelectric thin films through displacement measurements of cantilever-shaped piezoelectric structures. The displacement is measured using a laser Doppler vibrometer (LDV) under the applied electric field. Additionally, simple measurement results and analysis using this setup are presented.

2. EXPERIMENTAL SETUP FOR $e_{31,f}$ OF PIEZOELECTRIC THIN FILMS

- Figure 5 illustrates a schematic diagram of the setup used to measure the displacement at the end of a piezoelectric thin film cantilever device under the application of voltage.
- The measurement equipment can be configured as shown in Figs. 5(a) or (b), depending on the type of device used to generate the input signal for applying voltage and storing/recording the measured displacement signal at the end of the cantilever with an LDV.
- Figure 5(a) is a schematic of measurement equipment consisting of a function generator, voltage amplifier (×10), LDV, and oscilloscope.
- The function generator generates the signal according to the desired measurement objective and inputs it into the voltage amplifier.
- The signal output from the monitoring terminal of the voltage amplifier is input into Ch1 of the oscilloscope. If the attenuation ratio of the monitoring terminal of the voltage amplifier is M : 1, the voltage applied to the piezoelectric thin film can be calculated as shown in Equation (3).

$$V\,(\mathrm{V}) = V_{\mathrm{Ch1}} \times M \tag{3}$$

Here, V represents the voltage applied to the sample, and V_{Ch1} refers to the monitor voltage of the voltage amplifier received by Ch1 of the oscilloscope (or the voltage applied from the function generator).

- The amplified voltage signal from the voltage amplifier is applied by connecting it to the top and bottom electrodes of the piezoelectric thin film of the cantilever sample.
- The cantilever bends due to the applied voltage signal, and the displacement at the end of the cantilever is measured using the LDV.
- The displacement changes at the end of the cantilever measured by the LDV can be recorded by inputting it into Ch2 of the oscilloscope from the analog voltage output terminal in LDV. The displacement at the end of the cantilever can be calculated using the recorded signal and

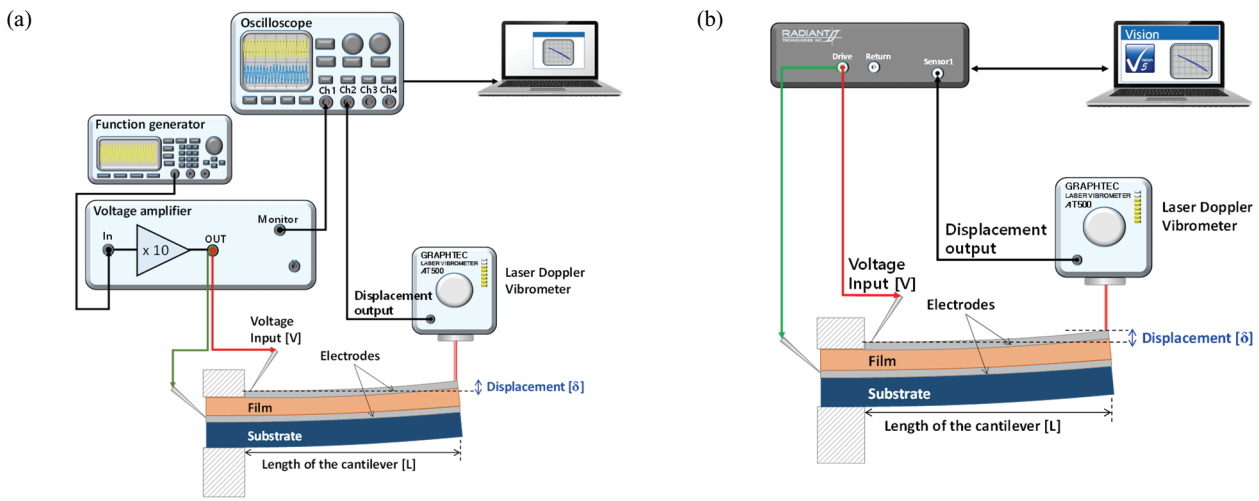

Fig. 5. Schematic diagram of the experimental setup for measuring the displacement at the end of a piezoelectric thin-film cantilever using an LDV. (a) A system consisting of a function generator, a voltage amplifier, an LDV, and an oscilloscope. (b) A system consisting of RADIANT's ferroelectric tester and an LDV. Adapted with permission from [28]. Copyright 2025 Tsinghua Univ Press.

Eq. (4). In Eq. (4), V_{Ch2} represents the displacement output signal of the LDV recorded in Ch2 of the oscilloscope. If the conversion ratio of the analog output signal is 10^{-6} m/V, the value from Ch2 can be converted to meters by multiplying it by 10^{-6}. Since the conversion ratio of the analog output signal varies by device, the ratio specified in the device's user manual should be used.

$$\text{Displacement } (\delta, \text{m}) = V_{Ch2} \times 10^{-6} \quad (4)$$

- LDVs are typical devices used for measuring vibration velocity. Depending on the equipment, analog voltage output for displacement might not be available, and only analog voltage output for velocity is provided. In such cases, as shown in Eq. (5), the analog voltage output signal for vibration velocity can be converted into an analog signal for displacement by integrating it over time using data processing software.

$$V_{x(t)} = \int V_{v(t)} dt \quad (5)$$

here, $V_{x(t)}$ and $V_{v(t)}$ represent the analog voltage output signals for displacement and velocity over time, respectively.

- $e_{31,f}$ can be calculated using Eq. (6). In Eq. (6), h_s is the thickness of the substrate (m), δ is the displacement at the end of the cantilever (m), $s_{11,s}$ is the elastic compliance of the substrate (m^2/N), L is the length of the cantilever (m), and V is the voltage applied to the piezoelectric thin film (V) [21].

$$e_{31,f} = \frac{d_{31}}{s^E_{11,p}} \cong -\frac{{h_s}^2}{3 s_{11,s} L^2} \frac{\delta}{V} \quad (6)$$

- Figure 5(b) is a schematic diagram of the measurement setup installed using the ferroelectric test equipment from RADIANT Technologies. INC.
- The ferroelectric test equipment from RADIANT Technologies. INC. allows for easy configuration of various input signals (bipolar loop, unipolar loop, double bipolar loop, double unipolar loop, fatigue test, etc.) using the dedicated software (Vision). It enables users to generate custom waveforms and easily create measurement programs, making it possible to develop batch programs for automated measurements under various measurement conditions.
- The voltage signal output from the Drive terminal of the ferroelectric test equipment from RADIANT Technologies. INC. is applied by connecting it to the top and bottom electrodes of the piezoelectric thin film on the cantilever sample. The displacement analog output terminal of the LDV is connected to the Sensor terminal of the RADIANT ferroelectric test equipment, facilitating the measurement of displacement in the piezoelectric thin film cantilever in response to the applied voltage.

3. EXAMPLE OF $e_{31,f}$ MEASUREMENT IN PIEZOELECTRIC THIN FILMS

- Figure 6 illustrates a schematic diagram of a sample fabricated by depositing $Bi_{1/2}Na_{1/2}TiO_3$-based thin films onto a $Pt/TiO_2/SiO_2/Si(100)$ substrates using the sol-gel method. The cantilever shape of the $Bi_{1/2}Na_{1/2}TiO_3$-based films are further processed to specific length and width. The prepared samples are subjected to voltage application while measuring the displacement of the cantilever using the measurement setup in Fig. 5(a). The applied voltage signal is a sinusoidal waveform with a voltage range of 0–30 V and a frequency of 100 Hz.
- Figure 7 is a graph of the data stored in Ch1 and Ch2 of the oscilloscope. When measuring the displacement of the cantilever using the LDV, noise from vibrations and sounds generated in the laboratory are also measured. To reduce the noise, it is necessary to install the sample holder and LDV on vibration isolation platforms and to provide

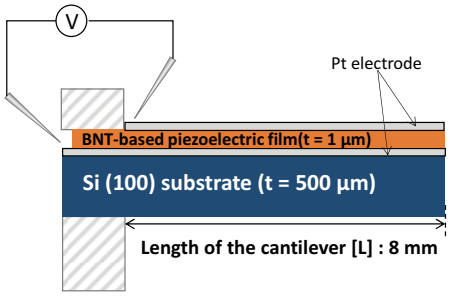

Fig. 6. Schematic diagram of the geometry of $Bi_{1/2}Na_{1/2}TiO_3$-based thin film cantilever deposited on $Pt/TiO_2/SiO_2/Si(100)$ substrates for measuring $e_{31,f}$.

soundproofing facilities. In general, LDV equipment typically includes built-in High Band Pass Filter and Low Band Pass Filter functions. For the GRAPHTEC AT500-05 LDV used in this study, the High Band Pass Filter can be set to 100 Hz, 10 Hz, or DC, while the Low Band Pass Filter can be set to 50 kHz, 10 kHz, or 1 kHz. These filter ranges can be configured by selecting the Band Pass Filter setup switches on the LDV unit. Nevertheless, if the noise caused by environmental vibrations and acoustic disturbances remains severe, the "Band Pass Filter" function in the data processing software can be used to further remove noise, as described below.

- Figure 8 is a screenshot of the step in the ORIGIN program (OriginLab) where the "FFT Filter" menu is opened to remove noise. By navigating through the menu bar: "Analysis" → "Signal processing" → "FFT filters" → "Open Dialog," the program menu opens, and as shown in Fig. 9, the "FFT Filters" window allows noise removal using the "Band Pass Filter."
- The procedure for removing noise using the "Band Pass Filter" is as follows:

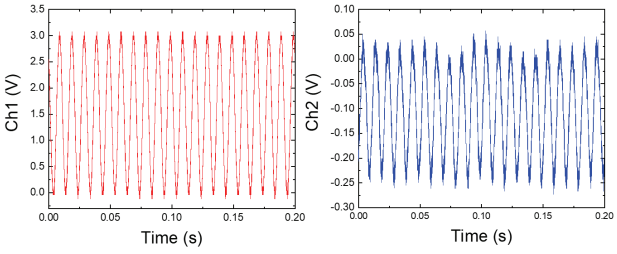

Fig. 7. Graphical representation of the signal stored on Ch1 and Ch2 of the oscilloscope after measurement using the measuring system of Fig. 5(a).

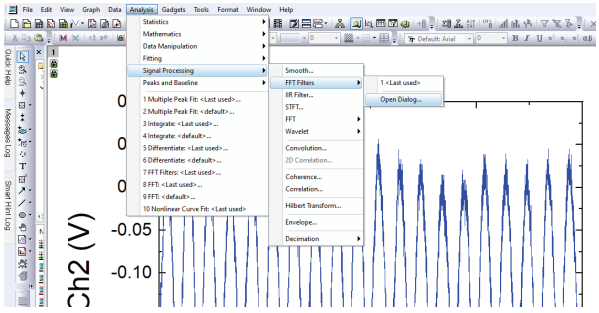

Fig. 8. Screen capture of the step of opening the "FFT filters" menu in the ORIGIN program (OriginLab) to remove noise.

① : Set the "Filter Type" to "Band Pass" in the menu (Fig. 9(a)).

② : Check the "Auto Preview" menu (Fig. 9(a)).

③ : Manually set the "Lower Cutoff Frequency" and "Upper Cutoff Frequency". Since the frequency of the applied voltage signal in this experiment is 100 Hz, setting the "Lower Cutoff Frequency" and "Upper Cutoff Frequency" around 100 Hz will result in a filtered signal as shown in Fig. 9(b).

④ : As in step ③, the "Lower Cutoff Frequency" and "Upper Cutoff Frequency" can be set by manually entering values, or the filtering frequency can be set by moving the dashed line on the Amplitude graph in the Preview window as shown in Fig. 9(c).

(a)

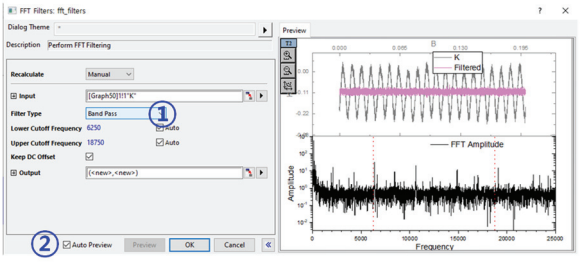

(b)

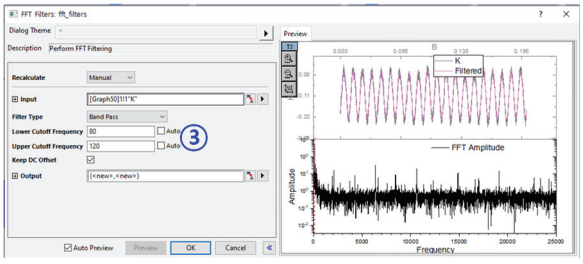

(c)

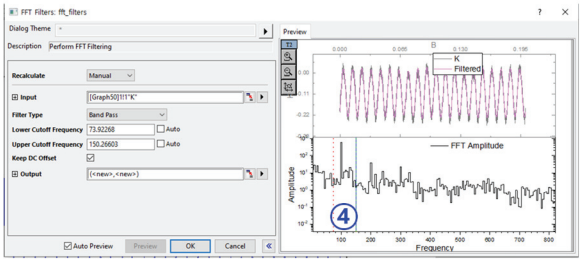

Fig. 9. Screen capture images of the scene where (a) "Band Pass Filter" and "Auto Preview" are set, (b) "Lower Cutoff Frequency" and "Upper Cutoff Frequency" are manually set, and (c) "Lower Cutoff Frequency" and "Upper Cutoff Frequency" are set by moving the dotted lines on the Amplitude graph in the Preview window. The "Lower Cutoff Frequency" and "Upper Cutoff Frequency" can be set by selecting either the steps in Figs. 9(b) or Fig. 9(c).

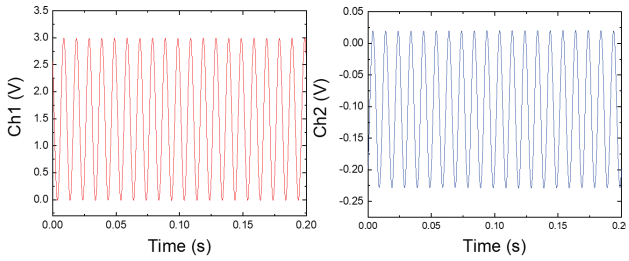

Fig. 10. Ch1 and Ch2 signals after removing noise using a band pass filter.

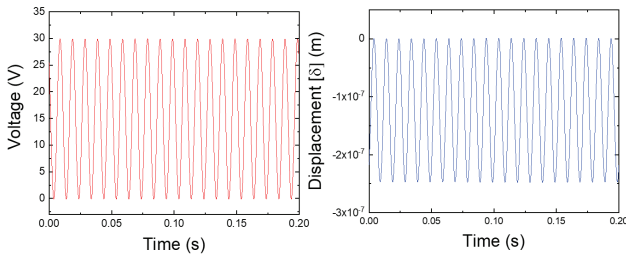

Fig. 11. Voltage and displacement graphs of noise-removed Ch1 and Ch2 signals converted using equations (3) and (4), respectively.

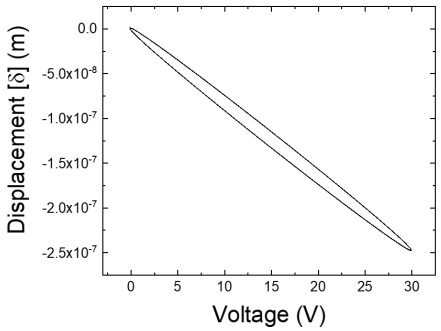

Fig. 12. Displacement-Voltage graph drawn using data obtained in Fig. 11.

Table 1. Information on cantilever material, applied voltage, and displacement values.

δ	Displacement (m)	-2.48×10^{-7}
V	Voltage (V)	30
h_s	Thickness of substrate (m)	5×10^{-4}
L	Sample length (m)	8×10^{-3}
$s_{11,s}$	Elastic compliance of substrate (m^2/N)	1.25×10^{2}

Table 2. Effective transverse piezoelectric coefficient $e_{31,f}$ (C/m^2) of piezoelectric thin films of representative lead-based and lead-free materials [21,27,29-32].

Category	Materials/Substrates	Crystalline quality	Thickness (μm)	Fabrication method	$e_{31,f}$ (C/m^2)	Ref.
Lead-based	PZT/Pt/TiO_2/SiO_2/Si	Polycrystalline	0.75	PLD	-14.3	[30]
	PZT/Pt/MgO (001)	Single domain	2.9	RF sputtering	-4.7 ~ -4.9	[21]
Lead-free	KNN/Pt/TiO_2/SiO_2/Si	Polycrystalline	0.75	PLD	-5.6	[31]
	KNMN/Pt/TiO_2/SiO_2/Si	Polycrystalline	1	Sol-gel	-8.5	[32]
	BNKT/Pt/TiO_2/SiO_2/Si	Polycrystalline	2	Sol-gel	-1.29 ~ -5.15	[27]
	$(Bi_{0.5}Na_{0.5})(Ti_{0.995}Mn_{0.005})O_3$/Pt/$TiO_2$/$SiO_2$/Si	Polycrystalline	1.12	Sol-gel	-2.43	[29]
	BNT-BA/Pt/TiO_2/SiO_2/Si	Polycrystalline	0.5	Sol-gel	-2.48	[28]

- Figure 10 is a graph of the data from Ch1 and Ch2 after removing noise using the "Band Pass Filter."
- Figure 11 is a graph of the input voltage and cantilever displacement, calculated using equations (3) and (4), from the data obtained after removing noise using the "Band Pass Filter."
- Figure 12 is the Displacement-Voltage graph plotted from the calculated input voltage and cantilever displacement data obtained from Fig. 11. When a 30 V voltage is applied to the cantilever-shaped $Bi_{1/2}Na_{1/2}TiO_3$-based thin film sample shown in Fig. 6, the displacement at the end of the cantilever was 2.48×10^{-7} m.
- The transverse piezoelectric coefficient $e_{31,f}$ of the $Bi_{1/2}Na_{1/2}TiO_3$-based piezoelectric thin film, calculated by

inputting the information from Table 1 into Equation (6), is -1.4 C/m^2.

- For reference, Table 2 summarizes the transverse piezoelectric properties of representative piezoelectric materials.

4. CONCLUSION

In conclusion, this tutorial has provided an in-depth overview of the experimental setup and methods for measuring the effective transverse piezoelectric coefficient $e_{31,f}$ of piezoelectric thin films using a laser Doppler vibrometer (LDV). The method outlined is a valuable tool for evaluating the piezoelectric properties of new materials and advancing the development of high-performance piezoelectric devices. The findings and techniques presented in this work will contribute to further research in the field of piezoelectric thin films and their applications in various technologies.

ORCID

Chang Won Ahn https://orcid.org/0000-0003-0613-9823

ACKNOWLEDGEMENTS

This research was supported by Basic Science Research Program (RS-2023-00245221) and Priority Research Centers Program (NRF-2019R1A6A1A11053838) through the National Research Foundation of Korea (NRF) funded by the Ministry of Education.

REFERENCES

[1] H. P. Kim, W. S. Kang, C. H. Hong, G. J. Lee, G. Choi, J. Ryu, and W. Jo, *Adv. Ceram. Energy Convers. Storage*, Edited by O. Guillon (Elsevier, 2020), p. 157.

[2] Y. Kwon, Y. Kim, H. Lee, and M. Ha, *J. Korean Inst. Electr. Electron. Mater. Eng.*, **38**, 1 (2025). doi: https://doi.org/10.4313/JKEM.2025.38.1.1

[3] M. S. Kim and S. S. Park, *J. Korean Inst. Electr. Electron. Mater. Eng.*, **34**, 487 (2021). doi: https://doi.org/10.4313/JKEM.2021.34.6.14

[4] H. Kang, H. Jeong, S. Hong, N. K. Yoon, and S. Sohn, *J. Korean Inst. Electr. Electron. Mater. Eng.*, **37**, 382 (2024). doi: https://doi.org/10.4313/JKEM.2024.37.4.4

[5] P. Regtien and E. Dertien, *Sensors for Mechatronics*, 2nd edn. (Elsevier, 2018), p. 245.

[6] S. P. Beeby, N. J. Grabham, and N. M. White, *Sens. Rev.*, **21**, 33 (2001). doi: https://doi.org/10.1108/02602280110380575

[7] N. Sezer and M. Koç, *Nano Energy*, **80**, 105567 (2021). doi: https://doi.org/10.1016/j.nanoen.2020.105567

[8] S. S. Won, M. Sheldon, N. Mostovych, J. Kwak, B. S. Chang, C. W. Ahn, A. I. Kingon, I. W. Kim, and S. H. Kim, *Appl. Phys. Lett.*, **107**, 202901 (2015). doi: https://doi.org/10.1063/1.4935557

[9] P. Joshi, S. Kumar, V. K. Jain, J. Akhtar, and J. Singh, *J. Microelectromech. Syst.*, **28**, 382 (2019). doi: https://doi.org/10.1109/JMEMS.2019.2908879

[10] M. A. Shah, I. A. Shah, D. G. Lee, and S. Hur, *J. Sens.*, **2019**, 9294528 (2019). doi: https://doi.org/10.1155/2019/9294528

[11] A. Fawzy, A. Magdy, and A. Hossam, *Alex. Eng. J.*, **61**, 3175 (2022). doi: https://doi.org/10.1016/j.aej.2021.08.044

[12] M. A. Dubois and P. Muralt, *Sens. Actuator A Phys.*, **77**, 106 (1999). doi: https://doi.org/10.1016/s0924-4247(99)00070-9

[13] M. P. Garcia, D. Gibson, D. A. Hughes, and C. G. Nuñez, *Adv. Phys. Res.*, **3**, 2300091 (2023). doi: https://doi.org/10.1002/apxr.202300091

[14] J. Chu, Z. Wang, and R. Maeda, *Jpn. J. Appl. Phys.*, **38**, L1482 (1999). doi: https://doi.org/10.1143/JJAP.38.L1482

[15] G. Tan, K. Maruyama, Y. Kanamitsu, S. Nishioka, T. Ozaki, T. Umegaki, H. Hida, and I. Kanno, *Sci. Rep.*, **9**, 7309 (2019). doi: https://doi.org/10.1038/s41598-019-43869-1

[16] J. M. Liu, B. Pan, H. L. W. Chan, S. N. Zhu, Y. Y. Zhu, and Z. G. Liu, *Mater. Chem. Phys.*, **75**, 12 (2002). doi: https://doi.org/10.1016/S0254-0584(02)00023-8

[17] T. Furukawa, *IEEE Trans. Dielectr. Electr. Insul.*, **24**, 375 (1989). doi: https://doi.org/10.1109/14.30878

[18] T. Furukawa, J. Aiba, and E. Fukada, *J. Appl. Phys.*, **50**, 3615 (1979). doi: https://doi.org/10.1063/1.326310

[19] V. Giurgiutiu, *Structural Health Monitoring with Piezoelectric Wafer Active Sensors*, 2nd edn. (Academic Press, 2014), p. 21.

[20] V. V. KochervinskiĬ, *Crystallogr. Rep.*, **48**, 649 (2003). doi: https://doi.org/10.1134/1.1595194

[21] I. Kanno, H. Kotera, and K. Wasa, *Sens. Actuator A Phys.*, **107**, 68 (2003). doi: https://doi.org/10.1016/S0924-4247(03)00234-6

[22] J. W. Burssens, A. V. D. Wiel, and M. Kraft, *IEEE Trans.*

Instrum. Meas., **72**, 1 (2023).
doi: https://doi.org/10.1109/tim.2023.3268486

[23] J. F. Shepard, F. Chu, I. Kanno, and S. Trolier-McKinstry, *J. Appl. Phys*., **85**, 6711 (1999).
doi: https://doi.org/10.1063/1.370183

[24] J. F. Shepard Jr., P. J. Moses, and S. Trolier-McKinstry, *Sens. Actuator A Phys*., **71**, 133 (1998).
doi: https://doi.org/10.1016/S0924-4247(98)00161-7

[25] K. Prume, P. Muralt, F. Calame, T. Schmitz-Kempen, and S. Tiedke, *IEEE Trans. Ultrason. Ferroelectr. Freq. Control*, **54**, 8 (2007).
doi: https://doi.org/10.1109/tuffc.2007.206

[26] A. Mazzalai, D. Balma, N. Chidambaram, R. Matloub, and P. Muralt, *J. Microelectromech. Syst*., **24**, 831 (2015).
doi: https://doi.org/10.1109/JMEMS.2014.2353855

[27] S. A. Chae, S. S. Won, H. J. Seog, A. Ullah, C. W. Ahn, and I. W. Kim, *Curr. Appl. Phys*., **16**, 429 (2016).
doi: https://doi.org/10.1016/j.cap.2016.01.008

[28] M. Sheeraz, S. S. Won, J. P. Kim, S. Ali, F. Akram, H. S. Han, B. C. Park, T. H. Kim, I. W. Kim, A. Ullah, and C. W. Ahn, *J. Adv. Ceram.*, 2025.
doi: https://doi.org/10.26599/JAC.2025.9221034

[29] B. T. Nguyen, S. S. Won, B. C. Park, Y. J. Jo, C. W. Ahn, I. W. Kim, and T. H. Kim, *Curr. Appl. Phys*., **20**, 1447 (2020).
doi: https://doi.org/10.1016/j.cap.2020.07.004

[30] M. D. Nguyen, M. Dekkers, E. P. Houwman, H. T. Vu, H. N. Vu, and G. Rijnders, *Mater. Lett.*, **164**, 413 (2016).
doi: https://doi.org/10.1016/j.matlet.2015.11.044

[31] I. Kanno, T. Ichida, K. Adachi, H. Kotera, K. Shibata, and T. Mishima, *Sens. Actuator A Phys*., **179**, 132 (2012).
doi: https://doi.org/10.1016/j.sna.2012.03.003

[32] S. S. Won, J. Lee, V. Venugopal, D. J. Kim, J. Lee, I. W. Kim, A. I. Kingon, and S. H. Kim, *Appl. Phys. Lett.*, **108**, 232908 (2016).
doi: https://doi.org/10.1063/1.4953623